PILOT SEQUENCE DESIGN FOR TELEMETRY WAVEFORMS IN MULTI-ANTENNA TRANSMITTERS

PILOT SEQUENCE DESIGN FOR TELEMETRY WAVEFORMS IN MULTI-ANTENNA TRANSMITTERS

Oussama AIT SIDI ALI
SAFRAN DATA SYSTEMS
Les-Ulis, FRANCE
oussama.ait-sidi-ali@safrangroup.com

Alain THOMAS
SAFRAN DATA SYSTEMS
Les-Ulis, FRANCE
alain-dominique.thomas@safrangroup.com

Bertrand LE GAL
IRISA Laboratory
Lannion, FRANCE
bertrand.le-gal@irisa.fr

Romain TAJAN
IMS Laboratory
Bordeaux, FRANCE
romain.tajan@ims-bordeaux.fr

30/06/2025

ABSTRACT

In multi-antenna systems, accurate Channel State Information estimation is crucial for reliable data decoding. In aeronautical telemetry, the spatial separation of antennas onboard aircraft, which can span several meters, introduces non negligible differential delays between received signals at receiver side which degrades channel estimation, thereby impacting the communication performance. To address this issue, we propose to use Space Time Coding to generate pilot sequences that mitigate differential delay degradation. Thus leading to improved receiver robustness in multi-antenna aircraft telemetry systems. Complete communication system simulation using AWGN channel showcases gains in CSI estimation up to 6dB without any increase in pilot sequence size nor in computational complexity.

INTRODUCTION

Aeronautical telemetry plays a crucial role in flight testing, where real-time data transmission from onboard sensors to ground stations enables the evaluation of aircraft performance. However, maintaining a reliable communication link is challenging due to link outages caused by antenna masking from the aircraft's body. To mitigate this issue, a form of spatial diversity is typically employed. However, using only space diversity, where the same signal is transmitted from multiple antennas, can lead to destructive interference at the receiver due to phase differences between signals arriving via different paths as represented in Figure 1. This necessitates the use of an additional diversity dimension to ensure reliable transmissions.

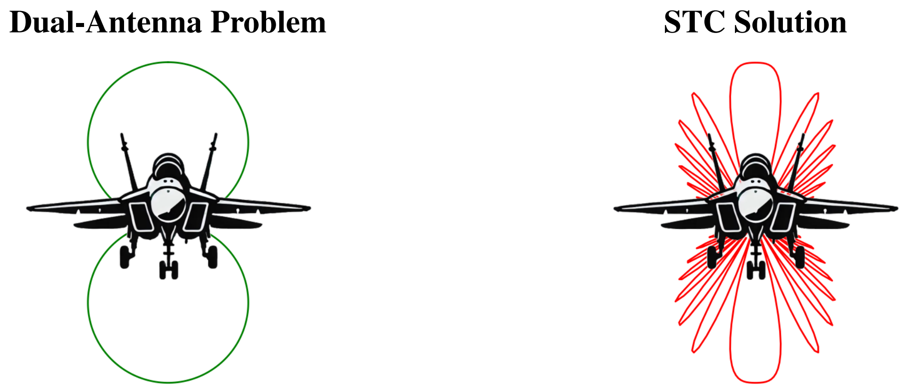

Figure 1: Radiation pattern for ideal dipole antennas.

The IRIG-106 telemetry standard promotes Space-Time Coding (STC) as a form of spatial diversity that improves link reliability without increasing spectral occupancy—unlike Space-Frequency diversity, which requires additional bandwidth. This makes STC especially suitable for bandwidth-constrained aeronautical telemetry. However, antenna separation introduces differential delays between received signals, which can degrade system performance.

In multi-antenna systems [8], Channel State Information (CSI) estimation typically relies on orthogonal pilot sequences. Differential delays caused by antenna spacing disrupt this orthogonality, reducing receiver accuracy. To mitigate this, we redesign pilot sequences to account for delay, preserving orthogonality. Simulations demonstrate that this method significantly outperforms IRIG-106 pilots, offering a more robust solution for multi-antenna telemetry systems.

PROBLEM FORMULATION

Achieving an optimal trade-off between spectral efficiency, power efficiency and system complexity is a crucial task in the aeronautical telemetry field. Among the various options provided by the IRIG-106 standard [9], the Shaped Offset Quadrature Phase Shift Keying - Telemetry Group (SOQPSK-TG) waveform stands out for its superior balance, making it a preferred choice for addressing the complex communication challenges in the aeronautical domain [1]. The STC scheme described by the IRIG-106 uses a 2-Tx/1-Rx antenna configuration with an Alamouti-like code.

A. Overview of Space-Time coded SOQPSK-TG

The SOQPSK-TG signal can be expressed in terms of its phase component [4], which is a function of the input data sequence. Originating from a Non Return to Zero (NRZ) coded bit sequence $\underline{b} = \{b_k\}_{k\in Z}$, with $b_k \in \{-1, 1\}$, a ternary sequence $\underline{\alpha} = \{\alpha_k\}_{k\in Z}$, with $\alpha_k \in \{-1, 0, 1\}$, is constructed [2]. Thus the continuous phase of the SOQPSK-TG signal, $\phi(t)$, evolves as:

$$s(t, \underline{\alpha}) = \exp\left(j\pi h \sum_{i=-\infty}^{\infty} \alpha_i q(t - iT)\right) \tag{1}$$

with T the symbol period. The received signal resulting from the propagation of the two

SOQPSK-TG STC signals $s_0(t)$ and $s_1(t)$ through the channel can be expressed as:

$$r(t) = [h_0 s_0(t - \tau_0) + h_1 s_1(t - \tau_1)]\, e^{j\omega_0 t} + n(t), \tag{2}$$

where h_0 and τ_0 (resp. h_1 and τ_1) are the complex gain factors and transmission delays of signal 0 (resp. of signal 1), with ω_0 the mean frequency offset and $n(t)$ denotes the Additive White Gaussian Noise (AWGN).

B. Pilot Signal Based CSI Estimation

In multi-antenna systems, accurate CSI estimation is essential for decoding transmitted data. This estimation typically relies on detecting known pilot sequences embedded in the transmitted signal [7] [3] [10]. For SOQPSK-TG STC, it is commonly performed using a two-correlator scheme, where each correlator matches a specific pilot sequence transmitted from different antennas. The correlator outputs for a received signal $r(t)$ are expressed as:

$$L_i(t) = |R_{r,s_{pi}}(0)| = |\int r(t)\, s^*_{pi}(t)\, dt| \tag{3}$$

where $R_{r,s_{pi}}$ is the correlation operator between the received signal and s_{pi}, it being the modulated pilot signal from antenna i. When properly designed, the pilot sequences ensure that the correlator outputs are maximal at the instant each pilot signal is detected.

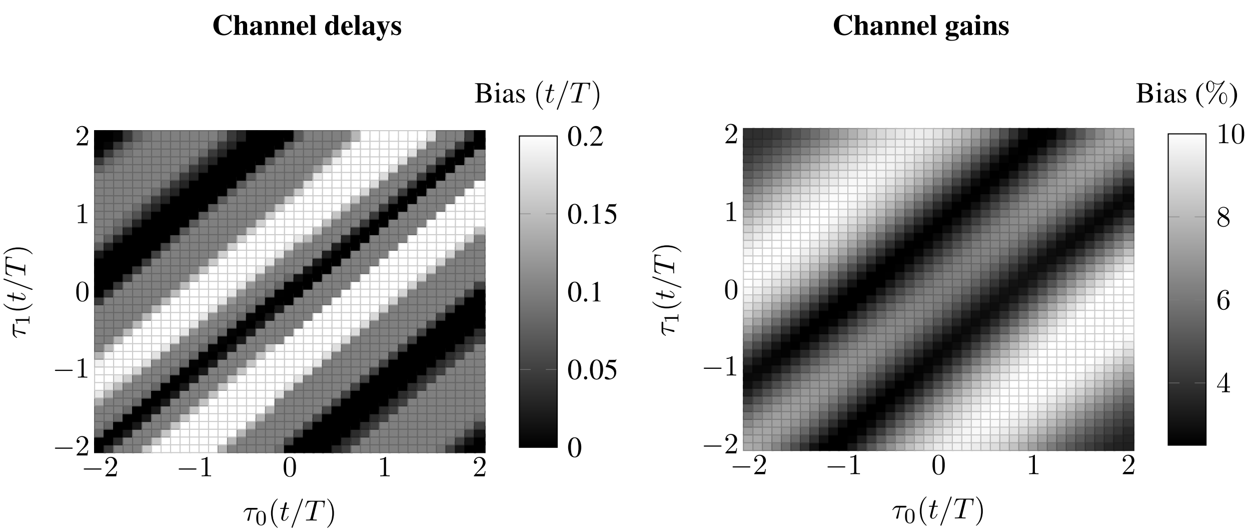

Figure 2: IRIG-106 pilot based CSI estimation error in a noiseless channel.

Simulations have shown that the IRIG-106 pilot sequences do not meet this criterion. Indeed, even in a noiseless channel, differential delay greatly impacts this scheme's performance as shown in Figure 2. These figures show that for different delay configurations, pilot detection can become biased by as much as $\frac{T}{5}$, which in return translates to up to a 10% bias in the complex channel gains estimation. As these biases in themselves are outside of the error margins described in [3], the SOQPSK-TG STC receiver's performance is degraded.

Thus we aim to present a process by which pilot sequences can be generated and optimized as to account for this differential delay. We'll also produce couples of pilot sequences that have been proven in simulation to mitigate differential delay, and thus improving the receiver's robustness.

SYSTEM MODEL

The Space-Time Block Code (STBC) used in the IRIG-106 standard [4] is derived from the Alamouti space time code [5], but applied to the OQPSK waveform [4]. The Alamouti scheme's transmit matrix M for a signal $a(t)$ can be written as follows:

$$M = \begin{array}{c} \begin{array}{cc} \text{Antenna 0} & \text{Antenna 1} \end{array} \\ \begin{bmatrix} a(2iT) & a((2i+1)T) \\ -a^*((2i+1)T) & a(2iT)^* \end{bmatrix} \end{array} \begin{array}{c} \\ t = 2iT \\ t = (2i+1)T \end{array} \tag{4}$$

By mapping the newly Alamouti encoded symbols a_0 and a_1 to the original bit stream $\underline{b}$, two new bit streams are constructed, $\underline{b^0}$ and $\underline{b^1}$:

$$b^0 = b \text{ . diag}(M_0, ..., M_0) \qquad\qquad b^1 = b \text{ . diag}(M_1, ..., M_1) \tag{5}$$

with b, b^0, b^1 row vectors, and M_0, M_1 the IRIG-106 Space Time Block Code (STBC) becomes:

$$M_0 = \begin{bmatrix} 1 & 0 & 0 & 0 \\ 0 & 1 & 0 & 0 \\ 0 & 0 & -1 & 0 \\ 0 & 0 & 0 & 1 \end{bmatrix} \quad M_1 = \begin{bmatrix} 0 & 0 & 1 & 0 \\ 0 & 0 & 0 & -1 \\ 1 & 0 & 0 & 0 \\ 0 & 1 & 0 & 0 \end{bmatrix} \tag{6}$$

This STBC can then be used to create the two SOQPSK-TG data streams, b_0 and b_1, to be transmitted from the two on-board antennas. The transmitted data is formatted by inserting 128 bit pilot sequences, p_0 and p_1 in the STBC bit streams periodically.

C. Pilot Detection

The state-of-the-art pilot detection scheme evaluates the correlations performed in (3) to detect either of the two modulated pilot sequences s_{p0} or s_{p1} within the received signal. The correlation between the received signal and each pilot sequence is primarily influenced by two factors: the autocorrelation characteristics of each individual pilot signal and the cross-correlation between the two distinct pilot sequences. When unbiased, a detection occurs when either autocorrelation terms is maximized. It can be shown that this is true at time $t - \tau_0$ and $t - \tau_1$ for each of the two correlations respectively.

$$L_{0,max} = |h_0 R_{s_{p0},s_{p0}}(0) + \underbrace{h_1 R_{s_{p1},s_{p0}}(\tau_1 - \tau_0)}_{\text{interfering term}}|, L_{1,max} \;\; = |h_1 R_{s_{p1},s_{p1}}(0) + \underbrace{h_0 R_{s_{p0},s_{p1}}(\tau_0 - \tau_1)}_{\text{interfering term}}| \tag{7}$$

However, equation 7 shows that a non-null cross-correlation between the two pilot signals can actually skew the pilot detection either by triggering it too soon or too late. Minimizing it is therefore a priority when it comes to pilot sequence design.

D. CSI estimation

CSI estimation is critical as it ensures the proper decoding and separation of the Alamouti-like encoded SOQPSK-TG signals received over the two channels. The maximum likelihood estimates

[3] of the delays and frequency offset are obtained by minimizing the residual error:

$$F(\hat{\tau_0}, \hat{\tau_1}, \hat{\omega_0}) = \left\| \mathbf{r} - \mathbf{\Omega} \mathbf{P} (\mathbf{P}^H \mathbf{P})^{-1} \mathbf{P}^H \mathbf{\Omega}^H \mathbf{r} \right\|^2. \tag{8}$$

The corresponding channel gains $\mathbf{h}$ are computed as:

$$\hat{\mathbf{h}} = (\hat{\mathbf{P}}^H \hat{\mathbf{P}})^{-1} \hat{\mathbf{P}}^H \mathbf{r}. \tag{9}$$

where $\mathbf{r}$ is the vector of received samples corresponding to the pilot signal. $\mathbf{\Omega}$ is a diagonal matrix defined by the frequency offset ω_0:

$$\mathbf{\Omega} = \text{diag}\left(1, e^{j\omega_0}, \ldots, e^{j(N_p-1)\omega_0}\right) \tag{10}$$

with N_p is the number of pilot samples. Finally, $\mathbf{P}$ is the pilot sequence matrix, which depends on the delays τ_0 and τ_1 for the two channels:

$$\mathbf{P} = \begin{bmatrix} s_{p0}(-\tau_0) & s_{p1}(-\tau_1) \\ s_{p0}(1-\tau_0) & s_{p1}(1-\tau_1) \\ \vdots & \vdots \\ s_{p0}(N_p-1-\tau_0) & s_{p1}(N_p-1-\tau_1) \end{bmatrix}, \tag{11}$$

where $\mathbf{h} = [h_0, h_1]^T$ represents the channel gains for the two channels. $\mathbf{n}$ is the noise vector.

E. Minimizing the Cramér-Rao Bound Through Pilot Sequence Orthogonality

As demonstrated in [6], the Cramér-Rao Bound (CRB), is given by the diagonal elements of the inverse Fisher Information Matrix (FIM):

$$crb(\hat{\mathbf{h}})^{-1} = \mathbf{J} = \frac{1}{\sigma^2} \tilde{\mathbf{P}}^T \tilde{\mathbf{P}} \qquad var(\hat{\mathbf{h}}) \geq \mathbf{J}^{-1} \tag{12}$$

$$\tilde{\mathbf{P}} = \begin{bmatrix} \Re\{\mathbf{P}\} & -\Im\{\mathbf{P}\} \\ \Im\{\mathbf{P}\} & \Re\{\mathbf{P}\} \end{bmatrix}$$

Minimizing the cross-correlation between pilot sequences, i.e., ensuring $\mathbf{s}_{p0}^H \mathbf{s}_{p1} \approx 0$ reduces the off-diagonal terms of $\mathbf{J}$, leading to a diagonal matrix. This, in turn, minimizes the CRB which improves the accuracy of channel gain estimation and enhances the receiver performance.

SPACE-TIME CODED PILOT SEQUENCES

This section details a trellis-based strategy for constructing Space-Time coded pilots, which tackles both the inherent memory effect in CPM waveforms and also potential differential delay.

F. Pilot Design Considerations for CPM Waveforms

In CPM systems such as SOQPSK-TG, each transmitted bit contributes energy to multiple symbols due to the continuous nature of the signal's phase trajectory. Thus resulting in inter-symbol dependencies. In Figure 4, one observes how the autocorrelation's main lobe spans several symbol periods. This memory effect implies that pilot design must carefully consider how bit patterns overlap in time. Consequently, simple zero-lag cross-correlation minimization becomes insufficient; *the relevant correlation extends across a finite temporal window*.

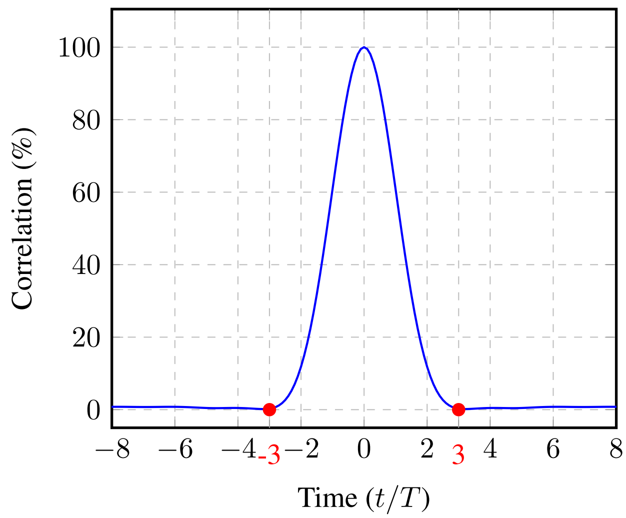

Figure 3: SOQPSK-TG autocorrelation function.

G. *Pilot Design Considerations for Differential Delay*

The asynchrony of the two transmitted signals can introduce an *additional* source of correlation between the pilot signals, as the delayed version of one antenna's signal may overlap more substantially with the other antenna's in time.

To handle this in pilot design, we extend the interval over which the cross-correlation is evaluated. In addition to considering the CPM memory window of $\pm 3T$, we incorporate the maximal differential delay $\Delta\tau_{\max}$. Hence, the relevant correlation metric is computed over

$$B_{s_{p0},s_{p1}} = \int_{-3T-\Delta\tau_{\max}}^{3T+\Delta\tau_{\max}} |R_{s_{p0},s_{p1}}(\tau)| \,\mathrm{d}\tau, \tag{13}$$

rather than just the $\pm 3T$ range. By widening the integration bounds, any potential overlap of delayed signals is reflected in the branch metric, ensuring that the pilot selection process accounts for *both* CPM memory *and* differential delay.

H. *Extended Alamouti Code*

We propose to generate Space-Time block coded pilot sequence couples. As STBCs have been proven to improve the orthogonality of the transmitted data (payload) signal, we propose to apply it to pilot sequences as well.

Table 1: Alamouti Space-Time Block Code Transmit Matrix with General Symbol Spacing

Alamouti type	**Time Slot**	**Antenna 1**	**Antenna 2**
Canonical	t	$s(n)$	$s(n+1)$
	$t+T$	$-s^*(n+1)$	$s^*(n)$
Time Extended	t	$s(n)$	$s(n+N)$
	$t+NT$	$-s^*(n+N)$	$s^*(n)$

A key step in our approach is to generalize the canonical Alamouti transmit matrix to accommodate non-adjacent symbol pairs. Thus, we create new STBCs matrices of size $4Nx4N$ from the extended Alamouti code :

$$M_0^N = \begin{bmatrix} \begin{bmatrix}1 & 0\\0 & 1\end{bmatrix} & \mathbf{0} & \mathbf{0} & \mathbf{0} & \cdots & \mathbf{0} \\ \mathbf{0} & \ddots & \mathbf{0} & \mathbf{0} & \cdots & \mathbf{0} \\ \mathbf{0} & \mathbf{0} & \begin{bmatrix}1 & 0\\0 & 1\end{bmatrix} & \mathbf{0} & \cdots & \mathbf{0} \\ \mathbf{0} & \mathbf{0} & \mathbf{0} & \begin{bmatrix}-1 & 0\\0 & 1\end{bmatrix} & \mathbf{0} & \mathbf{0} \\ \cdots & \cdots & \cdots & \mathbf{0} & \ddots & \mathbf{0} \\ \mathbf{0} & \mathbf{0} & \mathbf{0} & \mathbf{0} & \mathbf{0} & \begin{bmatrix}-1 & 0\\0 & 1\end{bmatrix} \end{bmatrix} \begin{matrix} \left.\begin{matrix} \\ \\ \\ \end{matrix}\right\} N \text{ times} \\ \left.\begin{matrix} \\ \\ \\ \end{matrix}\right\} N \text{ times} \end{matrix} \tag{14}$$

$$M_1^N = \begin{bmatrix} \mathbf{0} & \cdots & \mathbf{0} & \mathbf{0} & \mathbf{0} & \begin{bmatrix}1 & 0\\0 & -1\end{bmatrix} \\ \mathbf{0} & \cdots & \mathbf{0} & \mathbf{0} & \iddots & \mathbf{0} \\ \mathbf{0} & \cdots & \mathbf{0} & \begin{bmatrix}1 & 0\\0 & -1\end{bmatrix} & \mathbf{0} & \mathbf{0} \\ \mathbf{0} & \mathbf{0} & \begin{bmatrix}1 & 0\\0 & 1\end{bmatrix} & \mathbf{0} & \mathbf{0} & \mathbf{0} \\ \mathbf{0} & \iddots & \mathbf{0} & \mathbf{0} & \cdots & \mathbf{0} \\ \begin{bmatrix}1 & 0\\0 & 1\end{bmatrix} & \mathbf{0} & \mathbf{0} & \mathbf{0} & \mathbf{0} & \mathbf{0} \end{bmatrix} \begin{matrix} \left.\begin{matrix} \\ \\ \\ \end{matrix}\right\} N \text{ times} \\ \left.\begin{matrix} \\ \\ \\ \end{matrix}\right\} N \text{ times} \end{matrix} \tag{15}$$

Applying the STBC to a seed pilot sequence significantly reduces the complexity of the search process. Traditionally two separate 128-bit pilot sequences $\mathbf{p}_0$ and $\mathbf{p}_1$ need to be designed independently. This results in a search space of size 2^{256}. However, through this method only a single 128-bit pilot sequence $\mathbf{p}$ needs to be generated, thanks to which the two required pilot sequences can be obtained through the STBC.

I. Proposed Pilot Search Approach

Although focusing on one 128-bit pilot reduces the computational complexity, the remaining search space is still immense. To address this challenge, we decompose the sequence into segments of length $4N$ bits, each corresponding to a block of extended Alamouti encoding. Each segment $S(i)$, with $i = 1, \ldots, 2^{4N}$, can be viewed as a *state* in a trellis. We then define transitions $S(i) \rightarrow S(j)$ by concatenating bit patterns from $S(i)$ and $S(j)$. Space–time encoding these combined bits yields two signals, $s_0^{(i,j)}$ and $s_1^{(i,j)}$.

To rank each transition, we define the branch metric

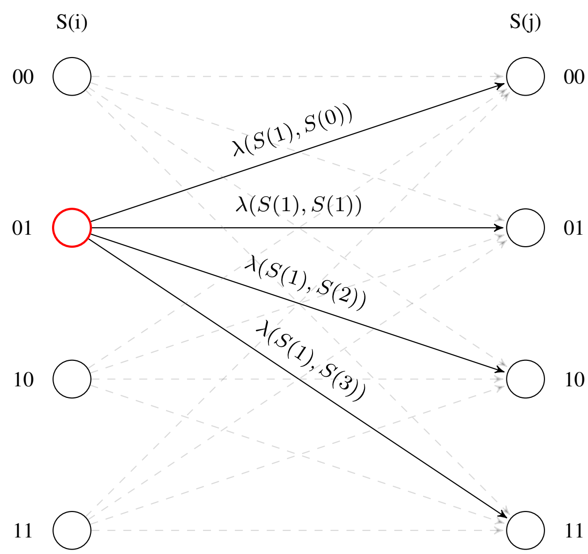

Figure 4: Trellis used to construct the look-up table for $N = 1$

$$\lambda\big(S(i), S(j)\big) \;=\; \int_{-3T-\Delta\tau_{\max}}^{3T+\Delta\tau_{\max}} \left|R_{s_0^{(i,j)},\, s_1^{(i,j)}}(\tau)\right| \mathrm{d}\tau, \tag{16}$$

where $\Delta\tau_{\max}$ is an upper bound on the differential delay. This integral captures *all* relevant correlation between $s_0^{(i,j)}$ and $s_1^{(i,j)}$ over the time window extended by both the CPM memory ($\pm 3T$) and the additional delay. Once the metric (16) is computed for all pairs $S(i)$, $S(j)$, we select for each $S(i)$ the best successor

$$\Gamma\big(S(i)\big) \;=\; \underset{S(j)}{\operatorname{argmin}}\, \lambda\big(S(i), S(j)\big) \tag{17}$$

Storing $\Gamma\big(S(i)\big)$ creates a look-up table enabling fast pilot construction. We start with an initial state $S(i)$, then repeatedly look up the best successor to grow the pilot in increments of $4N$ bits until reaching 128 bits.

We obtain 2^{4N} seed sequence candidates. Each candidate is evaluated using the same metric (13), across the entire pilot length. Repeating the procedure for different N values (e.g. $N = 1, 2, 3, 4$) allows further tuning of the symbol gap to match system needs. Doing so reduces the search overhead while retaining the *performance benefits* of extended Alamouti coding in the presence of CPM memory and differential delay.

NUMERICAL RESULTS

J. SOQPSK-TG STC pilot correlation

The first numerical simulations were performed using a noiseless channel model with 128 bits long pilot sequences. Figure 5 compares the cross-correlation values of pilot sequences generated by the approach described in Section IV for $N = 1, 2, 3, 4$ alongside IRIG-106 as a reference. For $N \geq 2$, our pilot sequences achieve lower cross-correlations in the relevant lag region. Thus also showing that increasing the spacing parameter N within the extended Alamouti framework mitigates memory overlaps more effectively.

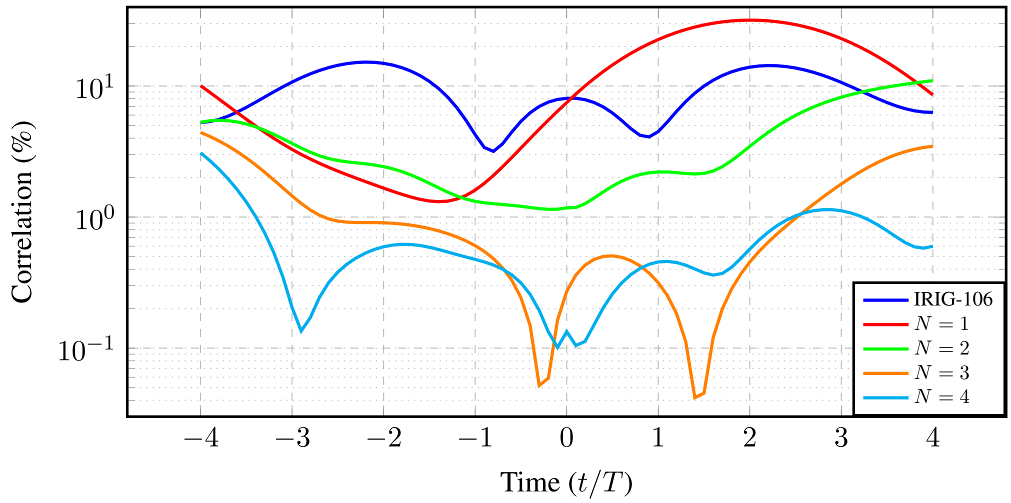

Figure 5: Cross-correlation values for different pilot sequences.

K. SOQPSK-TG STC CSI estimation

Similar simulations to the ones whose results are showcased in Figure 2 have been performed with the following sequences generated with $N = 4$:

$$\mathbf{p} = (417C21140364B9D6782B243FFBD084FF)_{16} \tag{18}$$

IRIG-106 constrains $\Delta\tau_{max} = T$. Under this constraint, Figure 6 show the absence of any bias on the pilot detection as well as a maximum of 1.5% bias on the channel gains estimation using the space-time block coded sequences. Thus outperforming the IRIG-106 pilots.

To evaluate the performance gains provided by these new sequences in a complete system, we simulated the communication chain described in [3] and [2]. We performed Monte Carlo

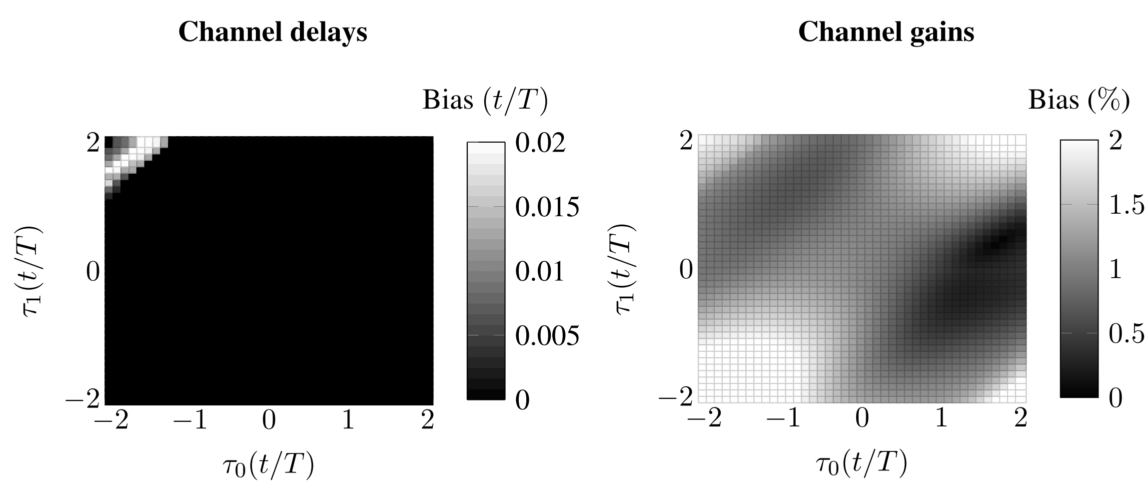

Figure 6: Complex gains estimation errors ($N = 4$ sequence)

simulations with AWGN noise and a differential delay ramp varying from $-T$ to T. The results obtained are presented in Figure 7. The Root Mean Squared Error (RMSE) of CSI estimation using the proposed pilot sequences show better accuracy than the IRIG-106 ones.

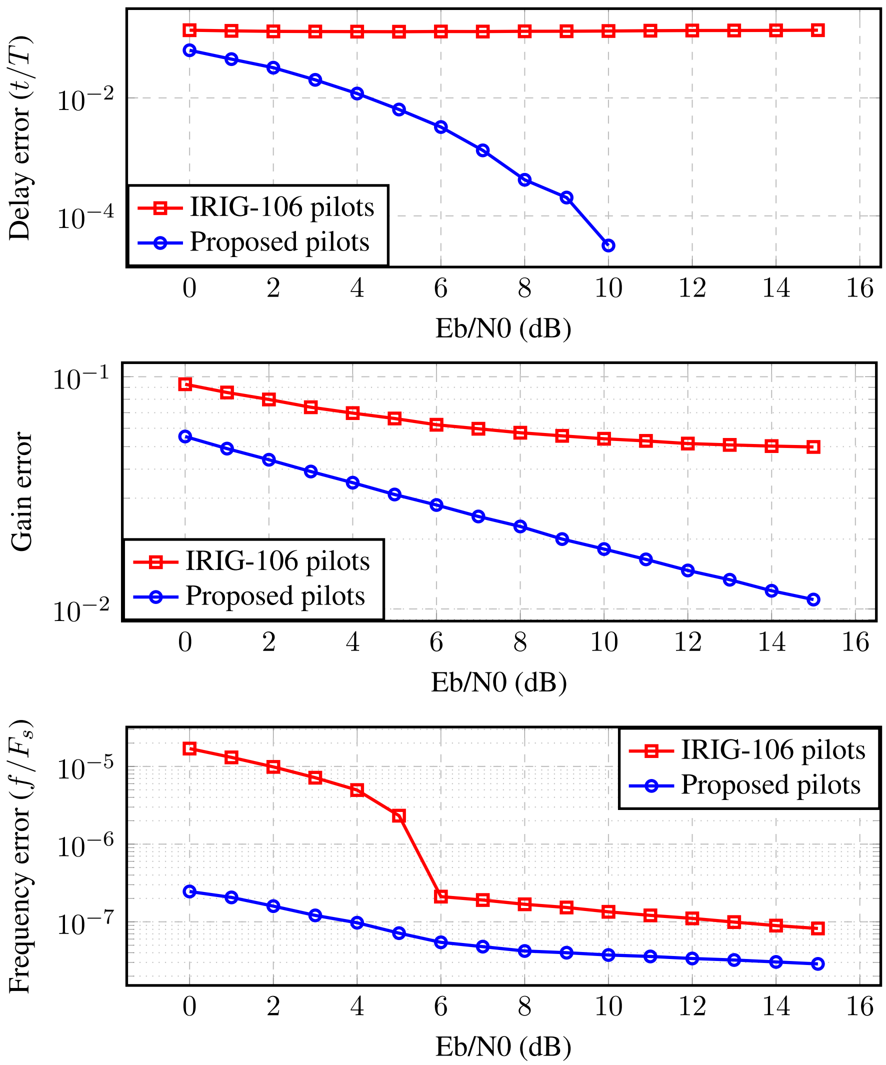

Figure 7: Simulated Root-Mean-Squared Error performance for CSI estimation vs Eb/N_0, for $h_0 = \sqrt{0.5}, h_1 = -\sqrt{0.5}$, $f_0 = 3kHz$, a sampling frequency $F_s = 80MHz$ and $\Delta\tau \in [-T, T]$.

CONCLUSIONS

In this paper, we addressed CSI estimation degradation using the IRIG-106 standard pilot sequences by focusing on their poor cross-correlation properties. We introduced a STBC-based pilot sequence design, supported by a strategy to navigate the large design space (2^{128}). Simulations confirmed the superiority of our sequences over IRIG-106 ones, showcasing significantly improved cross-correlation. Full-system simulations showed gains reflecting that, underscoring the effectiveness of our approach without increasing hardware complexity.

REFERENCES

[1] M.Geoghegan, L.Boucher, ”Space-Time Coding Solution to the Two-Antenna Interference Problem”, Int. Telemetering Conference, 2014.

[2] O.Rami, ”Study of Reception Techniques for Aeronautical Telemetry Modulations”, 2019.

[3] M.Rice, J.Palmer, C.Lavin, T.Nelson, ”Space-Time Coding for Aeronautical Telemetry: Part I—Estimators”, IEEE Transactions on Aerospace & Electronic Systems, 2017.

[4] Telemetry Standards, IRIG Standard 106-15 (Part 1), Appendix S, 2015.

[5] S.M. Alamouti, ”A Simple Transmit Diversity Technique for Wireless Communication”, IEEE Journal on Selected Areas in Communication, Vol 16, No, 8, October 1998.

[6] W.Harrison, M.Rice, S.Giddens, C.Josephson, ”Pilot Sequence Design for Space-Time Coded ARTM CPM”, International Telemetering Conference Proceedings, 2021.

[7] K.Pirabakaran, R.M.A.P. Rajatheva, ”Pilot Sequence Aided Channel Estimation For Space Time Coded Ofdm Systems”, Canadian Conf. on Electrical and Computer Engineering, 2005.

[8] M. Jensen, M. Rice, and A. Anderson, “Aeronautical telemetry using multiple-antenna transmitters,” IEEE Transactions on Aerospace and Electronic Systems, January 2007.

[9] Telemetry group, ”IRIG Telemetry Standard 106-20”, Secretariat Range Commanders Council US Army White Sands Missile Range, 2020.

[10] V.Romanuke, ”Improvement of Pilot Symbol Orthogonal Sequences in 2×2 to 4×4 MIMO Wireless Communication Systems with Channel State Estimation”, 2021.